Adaptive Independent Component Analysis-Based Clutter Filtering for Improved Non-Contrast Perfusion Ultrasound Imaging

Jaime Tierney[1], Don Wilkes[2], and Brett Byram[1]
[1]Department of Biomedical Engineering, Vanderbilt University, Nashville, TN, USA
[2]Department of Electrical Engineering and Computer Science, Vanderbilt University, Nashville, TN, USA

***Abstract*—Tissue motion makes perfusion ultrasound imaging without contrast difficult. We previously developed an adaptive demodulation (AD) method to correct for this motion prior to tissue filtering. Additionally, 2D space and time eigen-based clutter filtering has been shown to be superior to conventional frequency domain filtering performed only in the slow-time dimension, especially when long ensembles are used. We have shown that combining AD with singular value decomposition (SVD) filtering can improve slow blood flow detection. Here, we aim to develop and evaluate an adaptive independent component analysis (ICA) approach to clutter filtering and compare it to adaptive SVD filtering with and without AD using simulations and a single vessel phantom. We show that AD+ICA and ICA produce the highest blood-to-background signal-to-noise ratios in simulations and in the phantom, respectively.**

***Index Terms*—perfusion, adaptive demodulation, independent component analysis, singular value decomposition, power Doppler, ultrasound**

I. Introduction

Efficient tissue clutter filtering is challenging but crucial for ultrasound blood flow imaging. Without contrast, tissue needs to be filtered because blood signal is weaker than tissue and cannot be visualized. Tissue can also move at similar or greater velocities than perfusion or the slowest flow, causing a spectral overlap in the slow-time dimension [1]. This overlap makes conventional slow-time frequency domain filtering difficult. Additionally, conventional focused Doppler techniques are limited to small ensemble lengths, resulting in insufficient sampling for optimal tissue filtering [2].

To overcome these problems, several beamforming and post-processing advancements have been proposed. Among these is an adaptive tissue clutter demodulation (AD) technique that we previously developed to suppress the tissue clutter bandwidth prior to filtering [3]. Additionally, spatio-temporal singular value decomposition (SVD) filtering has been proposed in combination with plane wave synthetic focusing to overcome both the slow-time dimension and ensemble length limitations [4]. We previously showed that combining AD with an adaptive SVD filter [5] as well as plane wave synthetic focusing can further improve tissue clutter suppression, especially for smaller ensembles [6]. However, although the slow-time frequency-domain spectra overlap problem is better addressed with AD and SVD, tissue and blood principal components in the eigen-domain are not always distinct [7].

To overcome the eigen-domain overlap problem, we propose an adaptive independent component analysis (ICA) approach to tissue filtering in combination with the benefits of AD and plane wave synthetic focusing. ICA differs from SVD or principal component analysis (PCA) in that it identifies and separates based on higher order correlations that could otherwise cause principal components to overlap. ICA has been investigated previously in comparison to principal component analysis (PCA) methods and was shown to better separate tissue and blood [8]. However, ICA-based filtering has not yet been evaluated with other recent advancements in slow-flow ultrasound imaging. Furthermore, we propose an adaptive blood component selection reminiscent of the adaptive SVD approach proposed by Song et al. [5].

II. Methods

A. Theory and Implementation

We first assume a simple signal model, s, consisting of tissue, blood, and noise that is three dimensional in depth, lateral position, and time. Similar to SVD approaches, we start by reshaping s into a two dimensional casorati matrix, S, in space and time [4]. We then transpose S, take only the real part, and perform a singular value decomposition, $S = U\lambda V'$, where U and V are the temporal and spatial eigenvectors of S, respectively, and λ contains the singular values. We remove noise here using the same adaptive method as in Song et al. [5], such that $S_{tissue+blood} = U\lambda_{tissue+blood}V'$. To reduce dimensionality, we perform ICA on the spatial eigenvectors only, $S_s = \lambda_{tissue+blood}V'$.

ICA generally works by solving for two unknowns, A and D, such that $S_s = AD$. A is a square mixing matrix and D is our unmixed signal. ICA works by first solving for A, and then using A^{-1} to solve for D. Several techniques exist for solving for A. We use a maximum likelihood approach with BFGS optimization [9]–[11]. Once we solve for D, we can reconstruct blood using only the blood independent components in A and D, such that $S_{blood} = UA_{blood}D_{blood}$. Finally, we can transpose and reshape S_{blood} back to the original three dimensions in depth, lateral position, and time.

In this work, we developed an automated method for selecting the blood independent components using the energy of the components through time, $E = \sqrt{\frac{1}{T}\sum_t^T (UA)^2}$, sorted by

descending energy. Using two thresholds, we compute when the slope of E stops changing (from left to right) as well as when it starts to increase (from right to left). The mean of these two values is used as the cutoff between tissue and blood.

B. Simulations

A 0.5mm diameter vessel of blood scatterers within a 0.6 by 1cm area of tissue scatterers was constructed. Blood moved laminarly at a peak velocity of 1mm/s. Displacements estimated from hand motion phantom data were used to displace the tissue and blood scatterers to generate 6 realistic tissue motion realizations.

Field II [12] was used to simulate a 9-angle plane wave transmit sequence evenly spaced between -8° and 8°. A 7.8MHz frequency and PRF of 9kHz (1kHz frame rate) were used to acquire 1s of data. Channel data were beamformed using the method by Montaldo et al. [13].

AD was applied to all beamformed RF data as described in Tierney et al. [3], and tissue was filtered using both adaptive SVD and ICA. Adaptive SVD was implemented as in Song et al. [5], and adaptive ICA was implemented as described in the previous section.

C. Phantom

A polyvinyl alcohol and graphite mixture was used to make a phantom with a 0.6mm diameter vessel within a 2 by 3cm mold. After one freeze-thaw cycle, a syringe pump was used to flow blood mimicking fluid through the vessel at an average velocity of 1mm/s.

A Verasonics L12-5 probe was used to acquire plane wave channel data using the same transmit sequence that was used for simulations (1s, 9 angles, 7.8MHz frequency, 9kHz PRF). A volunteer held the probe during the acquisition to generate realistic tissue motion.

Channel data were beamformed and AD was applied the same way as was done for simulations. Different thresholds were used for SVD and ICA, but filtering was otherwise implemented the same as was done for simulations.

D. Image Quality Metrics

Power Doppler images were made by summing the squared filtered signal through slow-time. Blood-to-background signal-to-noise ratios (SNR) were computed as in Li et al. [14]. SNR was computed on power Doppler images made using ensembles between 20ms and 1s. B-mode and power Doppler images were log compressed and scaled to individual maximums and fixed dynamic ranges.

III. Results & Discussion

A. Simulations

Figure 1a shows simulated average blood-to-background SNR for ensemble sizes between 20ms and 1s for each filtering method with and without AD. AD+ICA produces the highest overall SNR when using a 400ms ensemble size. ICA and AD+ICA are more variable on average than SVD or AD+SVD, which have more consistent trends.

Figure 1b shows power Doppler images for an example realization at the 400ms ensemble for each filtering method with and without AD. Qualitatively, ICA and AD+ICA suppress background noise better than SVD. For this example, AD+SVD appears to make the vessel signal brighter and also suppresses the background noise better than SVD by itself. AD+ICA also appears to make the vessel brighter compared to ICA by itself, but ICA appears to suppress the background noise better than AD+ICA.

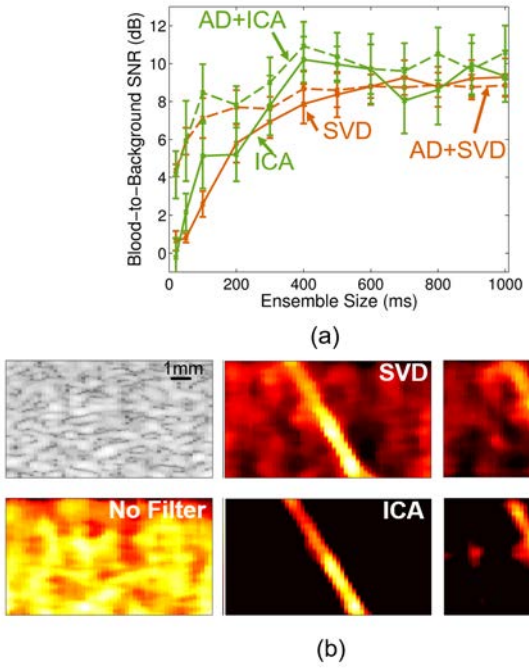

Fig. 1. (a) Average simulated blood-to-background SNR (± standard error) for each filtering method: SVD (solid orange), AD+SVD (dashed orange), ICA (solid green), AD+ICA (dashed green). (b) B-mode and power Doppler images for an example realization scaled to 60dB and 15dB, respectively.

B. Phantom

Figure 2a shows blood-to-background SNR for ensemble sizes between 20ms and 1s for each filtering method with and without AD for the phantom realization. ICA by itself produces the highest overall SNR when using a 400ms ensemble size. ICA and AD+ICA overall produce higher SNR than SVD and AD+SVD for larger ensemble sizes (above 300ms). AD+ICA produces the highest SNR for smaller ensemble sizes.

Figure 2b shows power Doppler images of the phantom using a 400ms ensemble for each filtering method with and without AD. Similar to the simulation results, qualitatively, ICA and AD+ICA suppress background noise better than SVD. For this realization, AD+SVD appears to suppress the background noise better than SVD. ICA by itself for this case suppresses the background noise the best.

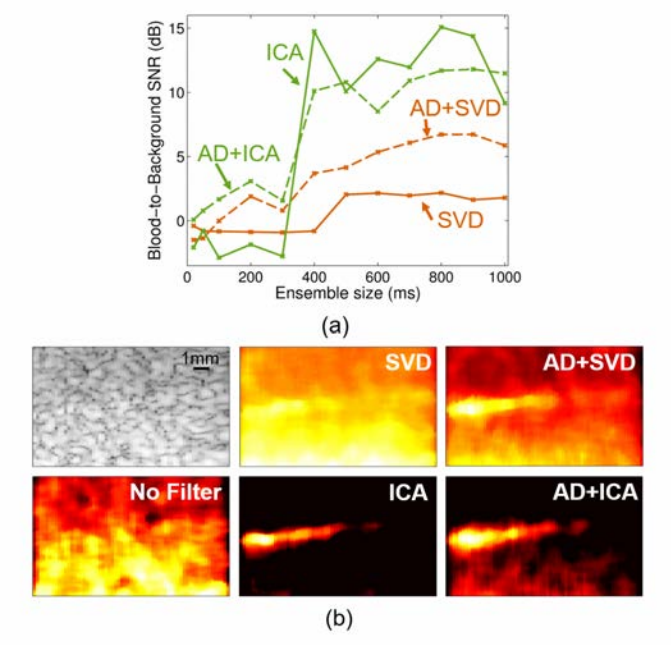

Fig. 2. (a) Average phantom blood-to-background SNR (± standard error) for each filtering method: SVD (solid orange), AD+SVD (dashed orange), ICA (solid green), AD+ICA (dashed green). (b) B-mode and power Doppler images for an example realization scaled to 60dB and 20dB, respectively.

IV. Conclusion

Tissue clutter filtering remains challenging when trying to image slow flow or perfusion. Several recent advancements in beamforming and tissue filtering have been proposed to improve tissue clutter suppression, including plane wave synthetic focusing, adaptive tissue clutter demodulation, and adaptive SVD filtering. Although ICA has been considered for tissue filtering in the past, it has yet to be evaluated in combination and in comparison to other recent advancements. Here, we developed an adaptive ICA-based tissue filtering approach and evaluated it in comparison to adaptive SVD with and without AD and with plane wave synthetic focusing. We demonstrate that adaptive ICA can improve blood-to-background SNR compared to adaptive SVD filtering.

Acknowledgment

The authors would like to thank the staff of the Vanderbilt University ACCRE computing resource. This work was supported in part by NIH grants 1R35HL135790-01 and S10OD016216-01 and NSF award IIS-1750994.

References

[1] A. Heimdal and H. Torp, "Ultrasound doppler measurements of low velocity blood flow: limitations due to clutter signals from vibrating muscles," *IEEE Transactions on Ultrasonics, Ferroelectrics and Frequency Control*, vol. 44, pp. 873–881, 1997.

[2] E. Mace, G. Montaldo, B. F. Osmanski, I. Cohen, M. Fink, and M. Tanter, "Functional ultrasound imaging of the brain: Theory and basic principles," *IEEE Transactions on Ultrasonics, Ferroelectrics, and Frequency Control*, vol. 60, pp. 492–506, 2013.

[3] J. Tierney, C. Coolbaugh, T. Towse, and B. Byram, "Adaptive clutter demodulation for non-contrast ultrasound perfusion imaging," *IEEE Transactions on Medical Imaging*, vol. 36, pp. 1979–1991, 2017.

[4] C. Demene, T. Deffieux, M. Pernot, B. F. Osmanski., V. Biran, S. Franqui, and M. Tanter, "Spatiotemporal clutter filtering of ultrafast ultrasound data highly increases doppler and fultrasound sensitivity," *IEEE Transactions on Medical Imaging*, vol. 34, pp. 2271–2285, 2015.

[5] P. Song, A. Manduca, J. D. Trzasko, and S. Chen, "Ultrasound small vessel imaging with block-wise adaptive local clutter filtering," *IEEE Transactions on Medical Imaging*, vol. 36, pp. 251–262, 2017.

[6] J. Tierney, M. George, C. Coolbaugh, T. Towse, and B. C. Byram, "Combining adaptive demodulation with singular value decomposition filtering for improved non-contrast perfusion ultrasound imaging," in *Proc. SPIE 10580, Medical Imaging 2018: Ultrasonic Imaging and Tomography*, Houston, TX, USA, March 2018.

[7] M. W. Kim, Y. Zhu, J. Hedhli, L. W. Dobrucki, and M. F. Insana, "Multi-dimensional clutter filter optimization for ultrasonic perfusion imaging," *IEEE transactions on ultrasonics, ferroelectrics, and frequency control*, 2018.

[8] C. Gallippi and G. Trahey, "Adaptive clutter filtering via blind source separation for two-dimensional ultrasonic blood velocity measurement," *Ultrasonic Imaging*, vol. 24, pp. 193–214, 2002.

[9] A. Bell and T. Sejnowski, "An information-maximization approach to blind separation and blind deconvolution," *Neural Computation*, vol. 7, pp. 1129–1159, 1995.

[10] H. Nielsen, "Ucminf - an algorithm for unconstrained, nonlinear optimization," IMM, Technical University of Denmark, Tech. Rep. IMM-TEC-0019, 2001. [Online]. Available: http://www.imm.dtu.dk/pubdb/views/edoc_download.php/642/ps/imm642.ps

[11] L. K. Hansen, J. Larsen, and T. Kolenda, "Blind detection of independent dynamic components," *In proc. IEEE ICASSP'2001*, vol. 5, pp. 3197–3200, 2001. [Online]. Available: http://www.imm.dtu.dk/pubdb/views/edoc_download.php/827/pdf/imm827.pdf

[12] J. A. Jensen, "Field: A program for simulating ultrasound systems," *Med. Biol. Eng. Comput.*, vol. 34, pp. 351–353, 1996.

[13] G. Montaldo, M. Tanter, J. Bercoff, N. Benech, and M. Fink, "Coherent plane-wave compounding for very high frame rate ultrasonography and transient elastography," *IEEE Transactions on Ultrasonics, Ferroelectrics, and Frequency Control*, vol. 56, pp. 489–506, 2009.

[14] Y. L. Li, D. Hyun, L. Abou-Elkacem, J. K. Willmann, and J. Dahl, "Visualization of small-diameter vessels by reduction of incoherent reverberation with coherent flow power doppler," *IEEE Transactions on Ultrasonics, Ferroelectrics, and Frequency Control*, vol. 63, pp. 1878–1889, 2016.